Title

Seismic waves increase permeability

Journal

Nature, 441

Authors

Elkhoury, Jean E.
Brodsky, Emily E.
Agnew, Duncan C.

Publication Date

2006-06-29

Peer reviewed

LETTERS

Seismic waves increase permeability

Jean E. Elkhoury[1], Emily E. Brodsky[2] & Duncan C. Agnew[3]

Earthquakes have been observed to affect hydrological systems in a variety of ways—water well levels can change dramatically, streams can become fuller and spring discharges can increase at the time of earthquakes[1–7]. Distant earthquakes may even increase the permeability in faults[8]. Most of these hydrological observations can be explained by some form of permeability increase[1,5]. Here we use the response of water well levels to solid Earth tides to measure permeability over a 20-year period. At the time of each of seven earthquakes in Southern California, we observe transient changes of up to 24° in the phase of the water level response to the dilatational volumetric strain of the semidiurnal tidal components of wells at the Piñon Flat Observatory in Southern California. After the earthquakes, the phase gradually returns to the background value at a rate of less than 0.1° per day. We use a model of axisymmetric flow driven by an imposed head oscillation through a single, laterally extensive, confined, homogeneous and isotropic aquifer to relate the phase response to aquifer properties[9]. We interpret the changes in phase response as due to changes in permeability. At the time of the earthquakes, the permeability at the site increases by a factor as high as three. The permeability increase depends roughly linearly on the amplitude of seismic-wave peak ground velocity in the range of 0.21–2.1 cm s^{-1}. Such permeability increases are of interest to hydrologists and oil reservoir engineers as they affect fluid flow and might determine long-term evolution of hydrological and oil-bearing systems. They may also be interesting to seismologists, as the resulting pore pressure changes can affect earthquakes by changing normal stresses on faults[10].

We use the response of wells to solid Earth tidal strains as a probe of the *in situ* permeability to provide a long-term, continuous record of permeability evolution[9,11,12]. The pressure in confined aquifers continually oscillates in response to the solid Earth tide. The volumetric strain of the Earth tide increases the pore pressure in the confined aquifer. Therefore, a pressure gradient is generated and the water flows in and out of the well, producing oscillations in water level. If the permeability of the aquifer is high, then the oscillations in the well are nearly in phase with the imposed tidal strain. If the permeability is low, then the water level oscillations lag significantly behind the solid Earth tidal strain as it takes some time for water to flow into the well. In between the extremes, there is a finite phase lag of the tidal oscillations in the well relative to the imposed tidal strain. The phase lags provide a means of measuring permeability.

In this study we consider water level data (Fig. 1) from two water wells in fractured granodiorite at Piñon Flat Observatory (PFO) in southern California (33.610° N, 116.457° W)[13]. The wells (CIB and CIC) are 300 m apart, and were drilled in 1981 to depths of 211 m and 137 m, respectively. Both are cased to 61 m and neither is pumped. Figure 1 shows the long-term water-level changes in these wells, driven in part by local precipitation; the inset shows the oscillations from the Earth tides. The dashed lines in Fig. 1 show the times of earthquakes (Fig. 2) that produced large shaking (see legend of Fig. 1).

We measure the phase shift of the water level relative to the dilatational strain for the semidiurnal tides (See Methods and Supplementary Information). Negative phases imply greater delay, so we refer to less negative phase shifts as smaller phase lags. As discussed above, the smallest lags (closest to zero) imply the highest permeabilities in the system.

Transient changes in the phase response are plainly seen in Fig. 3 at the times of all the earthquakes (dotted lines). Each transient change is characterized by a step in the phase response at the time of the earthquake followed by a gradual recovery of the phase to its pre-earthquake value. The phases recover linearly with time, though with different rates for the two wells: 0.08° per day for CIB and 0.04° per day for CIC.

We also evaluated the amplitude of the tidal response, which shows much smaller variations, especially in well CIC (see Supplementary

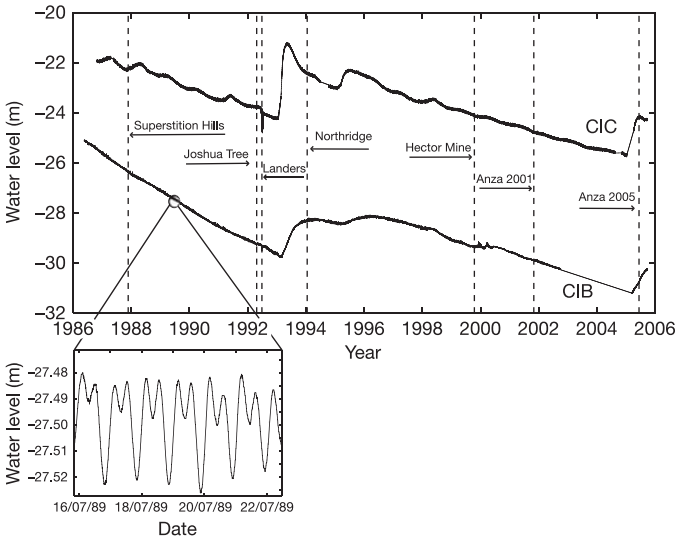

Figure 1 | Water level from wells CIB and CIC. Vertical dashed lines show the times of all earthquakes in the SCEC earthquake catalogue for Southern California (defined as 32° N–35° N; 119° W–114° W) with $M_L \geq 3$ that produced a synthetic Wood–Anderson amplitude of 1 m (~0.3 mm true ground motion at 1 Hz). This arbitrary threshold was chosen to provide a way to select earthquakes with large shaking systematically, because continuous on-scale seismic recording was not available at PFO for the entire study period. The set of seven earthquakes, which excludes aftershocks occurring within a month of the largest event, is robust to small differences in the M_L–distance relationship and the selection of earthquakes does not change even if the Wood–Anderson amplitude threshold is lowered to 0.5 m. Amplitudes are calculated from the magnitude–distance relationship of ref. 21. Long-term water-level changes are driven by local weather and seasonal rainfall. The oscillations in the inset are generated by Earth tides.

[1]Department of Earth and Space Sciences, University of California, Los Angeles, California 90095, USA. [2]Department of Earth Sciences, University of California, Santa Cruz, California 95060, USA. [3]Institute of Geophysics and Planetary Physics, Scripps Institution of Oceanography, University of California, San Diego, California 92093, USA.

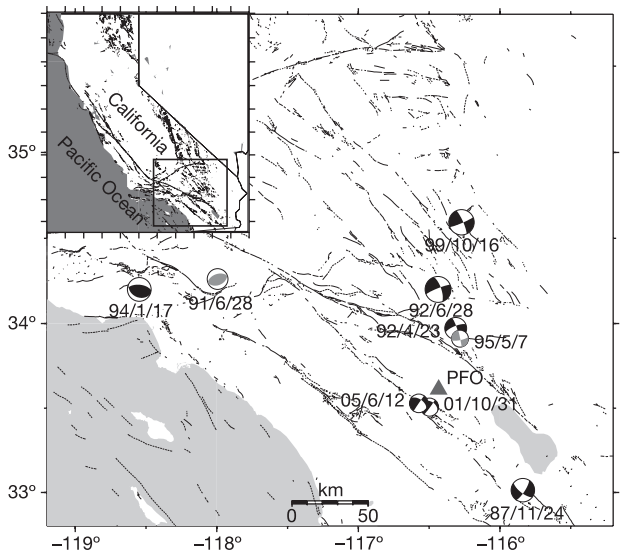

Figure 2 | Map of Southern California, showing epicentres of earthquakes considered in this study, as selected by the criterion in Fig. 1. The focal mechanisms of most earthquakes were obtained from the Hardebeck and Shearer catalogue[22]. The focal mechanisms of the Landers 92/6/28, Hector Mine 99/10/16 and Anza 05/6/12 earthquakes were obtained from the Harvard CMT catalogue because the Hardebeck and Shearer catalogue[22] does not include large events (Landers $M_w = 7.3$ and Hector Mine $M_w = 7.1$) or the latest earthquakes such as the Anza 2005 quake. The relative size of the beach ball symbols corresponds to the relative magnitudes of the earthquakes; 4.8 for the smallest and 7.3 for the largest. (For more information please see Supplementary Table S1.) Piñon Flat Observatory (PFO) is shown by a triangle. The light-shaded focal mechanisms show the two additional earthquakes described in the legend of Fig. 3.

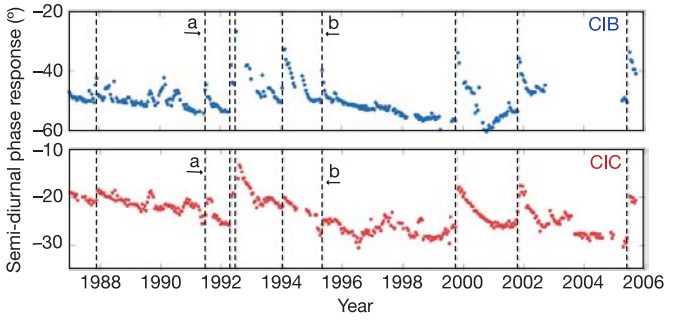

Figure 3 | Phase of the semidiurnal tide for the water level in the wells CIB and CIC, relative to the areal strain. Transient changes in the phase response are clearly shown at the time of the earthquakes (indicated as in Fig. 1) selected by the criterion in Fig. 1. Because our selection criterion is based on computed ground shaking at PFO, it missed at least two earthquakes: 'a' shows the 1991 Sierra Madre earthquake (PGV = 0.16 cm s^{-1}); and 'b' shows the 1995 Joshua Tree earthquake (PGV = 0.42 cm s^{-1}). These two additional earthquakes do not substantially affect the linear relationship between the permeability changes and the ground shaking defined by the set of seven earthquakes; see Fig. 4.

Information). The amplitude changes are relatively easily mapped into small storage changes and, unlike the phase, they are nearly insensitive to the permeability changes.

The observed changes at the times of the earthquakes imply that some earthquake-induced stress affected these well–aquifer systems. The change in static stress field and the dynamic stress from the seismic waves are both candidates. The static stress change for areal strain has the same sign as the first motion on seismograms, and for these earthquakes the first motions at PFO include both extension and compression. This is supported by calculations of static fields at PFO, which also show compression for Northridge and Anza 2001, but extension for all other earthquakes (Supplementary Table S1). But all earthquakes produced a decrease in the phase lag. Regardless of the detailed hydrological model, a phase lag decrease corresponds to an increase in permeability, which is unlikely to be produced by local compression and is extremely unlikely to be caused by both extension and compression. The dynamic, rather than static, strains are the probable cause, and we use the vertical peak ground velocity (PGV) as a proxy for the dynamic strain field[14] (Fig. 2). We measure the PGV directly from seismic records at PFO. The phase change is the difference between two measurements made before and after each earthquake over 200-h windows (see Supplementary Figs S3 and S4).

We quantitatively interpret aquifer phase lags as permeability (see the Methods section), following the methods of refs 9 and 3. Figure 4 plots the inferred changes in permeability at the time of the earthquakes against the PGV. For PGV values above 0.2 cm s^{-1}, the data show a linear relationship between the permeability change and the ground shaking:

$$\Delta k = R\frac{v}{c} \qquad (1)$$

where Δk is the change in permeability at the time of the earthquake, v is PGV in the vertical and c is the phase velocity of the seismic waves. The ratio v/c is approximately the imposed strain on the system[14], so R measures the permeability response to strain. The parameter R is a property of the well–aquifer system and is different for each well. Assuming c to be 3 km s^{-1}, $R_{CIB} \approx 3.0 \times 10^{-10}$ m^2 and $R_{CIC} \approx 8.4 \times 10^{-10}$ m^2.

We derived this relationship before the 2005 Anza earthquake, which generated the largest shaking at PFO yet recorded. This example provided a good opportunity to test equation (1). As can be seen in Fig. 4, the resulting permeability changes followed the linear trend previously defined by the other data points.

A commonly reported hydrological response to earthquakes is a drop in water level[3,4,5,11,15,16]. These Piñon Flat wells show water level drops for four of our study earthquakes. A key, unresolved problem is the relationship between these drops and the permeability enhancement recorded by the tidal phase change. We note that the tidal phase and the water level are sensitive to different regions of the well–aquifer system. The tidal phase averages the properties over an effective volume extending a distance of the order of $\sqrt{\kappa\tau}$ from the well, where κ is the hydrologic diffusivity (equal to the ratio of transmissivity and storage) and τ is the tidal period. For the hydraulic diffusivities that we infer from the PFO wells and the semidiurnal tidal period, this distance is of the order of 200 m. The two wells are 300 m apart, which is consistent with differing responses. On the other hand, persistent water level drops can record localized changes. Because of this difference, we are not surprised that the tidal response changes reveal a much more systematic relationship to PGV than is observed for water level changes in these wells.

To the best of our knowledge, the tidal responses measured here provide the first published long-term monitoring of permeability in a natural system. It is the first direct measurement of well-defined permeability increases in a natural setting before and after multiple earthquakes at the same site. It is also the first definitive relationship between measured permeability increases and other measured stresses in the field. The measurements led to a new and, to us, surprising conclusion. Permeability in a fractured rock system was increased significantly by the small stresses in seismic waves from regional earthquakes. The peak dynamic stress σ can be estimated from the PGV using the relationship $\sigma = \mu v/c$ where v is PGV, c is the phase velocity (as above) and μ is the shear modulus ($\sim 3 \times 10^{10}$ Pa), giving values in the range of 0.02 to 0.21 MPa for PGV in the range 0.2 to 2.1 cm s^{-1} (Fig. 2). (Previous studies[17] in intact laboratory samples had suggested that stresses of the order of 100 MPa were necessary to cause the large changes in the permeability that we observe.) The increases are systematic and even predictable. There is a roughly

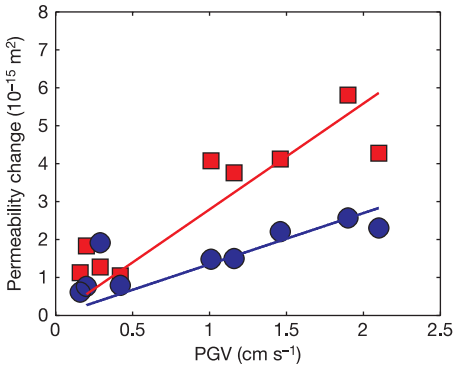

Figure 4 | Change in permeability for the well–aquifer systems CIB (circles) and CIC (squares) at the time of each of the earthquakes, plotted against peak ground velocity measured at PFO. Ground motion is low-passed at 0.5 Hz to make a comparable measurement on a variety of strong-motion and broadband seismometers. There is a linear relationship between the increase in permeability and the ground shaking for 0.2 to 2.1 cm s^{-1} peak ground velocities. We make a linear fit that goes through the origin to be consistent with the condition of no change in permeability in the absence of shaking. The slopes of the fit as described by equation (1) are $R_{CIB} = 3.4 \times 10^{-10}$ m^2 and $R_{CIC} = 8.4 \times 10^{-10}$ m^2. With the point for CIB from the Northridge earthquake removed, the goodness of fit r^2 is 0.7 (97% significance); with it included, r^2 for CIB is 0.3 and for CIC r^2 is 0.7 (see Supplementary Fig. S4). The average background permeability values are around 1.0×10^{-15} m^2 for CIB and 6.0×10^{-15} m^2 for CIC, giving a maximum increase by a factor of three for CIB and by a factor of two for CIC for the largest shaking.

linear relationship between the PGV and the permeability change at each well for the range of measured PGVs.

This result has potentially far-reaching consequences. First, we have demonstrated the utility of a simple, non-invasive method for monitoring permeability in confined aquifers or reservoirs. Second, the data indicate that relatively small dynamic stresses can double or triple permeability and therefore suggests a possible method for active permeability enhancement in economically useful geothermal, natural gas and oil reservoirs[18]. Third, the large variations of permeability over time indicate that natural permeability is not a fixed quantity, but rather an ever-evolving, dynamically controlled parameter. Fourth, and most speculatively, the fractures and flow resulting from such permeability-enhancement processes in faults might be a stage in the dynamic triggering of earthquakes[5,10].

METHODS

Tidal response. The phase and amplitude tidal responses were estimated using two separate methods which yielded nearly identical results. The measurements in Fig. 3 were derived using a least-squares fit of the observed water level data to the predicted tides based on a high-precision ephemeris (see Supplementary Information). As a check, we performed a second analysis in the frequency domain by dividing the Fourier transform of the observed tide and a synthetic tide, and taking the result at the frequency of the largest semidiurnal tide (M_2). The permeability changes are robust and the results are indistinguishable from the time-domain calculation.

Flow model. In estimating aquifer properties, we follow ref. 9 in modelling the tidal response as a result of flow in a single, laterally extensive, confined, homogeneous and isotropic aquifer. In an isotropic system, the far-field tidal head oscillation is proportional to the volumetric strain. In reality, it is unlikely that the aquifer is either homogeneous or isotropic. The most important omitted effect is the coupling of shear stresses to pore pressure by anisotropic fractures[19]. This complication would introduce a phase shift to all of our measurements and therefore bias our permeability estimates; however, the imposed phase shift should not change over time. The relative measurements we make using the Hsieh model[9] should be robust to these complications.

We corrected for the water table effect on the phase shift[3] by adding 15° to the observed lags. The semi-confined aquifer leaks, so this correction is necessary to account for the small amount of pore pressure diffusion to the free surface. The diffusion time of the leakage is known from the recovery time of water level drops after earthquakes. Once the diffusion time is known, we can calculate the leakage following ref. 3.

The well response depends on the flow of water through the porous medium and therefore is sensitive to the aquifer transmissivity and storage. Transmissivity is the rate of water transmission through a unit width of aquifer under a unit hydraulic gradient and is directly proportional to permeability. Storage is the strain change per unit imposed head and is a measure of compressibility.

Additional factors in the response in the most general case also include the well geometry, the period of the oscillation and inertial effects. The inertial effects are negligible for the long periods of the Earth tides[20]. The other two factors are independently well constrained.

The amplitude A and phase η responses for the long periods of tidal oscillations are[9]:

$$A = (E^2 + F^2)^{-\frac{1}{2}} \tag{2}$$

$$\eta = -\tan^{-1}(F/E) \tag{3}$$

where

$$E \approx 1 - \frac{\omega r_c^2}{2T}\mathrm{Kei}(\alpha), \quad F \approx \frac{\omega r_c^2}{2T}\mathrm{Ker}(\alpha), \quad \alpha = \left(\frac{\omega S}{T}\right)^{\frac{1}{2}} r_w \tag{4}$$

and T is the transmissivity, S the dimensionless storage coefficient, Ker and Kei the zeroth-order Kelvin functions, r_w is the radius of the well (8.8 cm for CIB, 9.1 cm for CIC), r_c is the inner radius of the casing (7.9 cm for both wells) and ω is the frequency of the tide.

We use the measured phase and the amplitude responses η and A with equations (2) and (3) to solve for storage and transmissivity. The storage shows only small (<40%) changes as a function of time. This result is a direct consequence of the lack of large variations in the amplitude response.

The relationship between transmissivity and permeability is:

$$k = \frac{\mu}{\rho g d} T \tag{5}$$

where k is the permeability, μ is the dynamic viscosity, ρ is the density, g is the gravitational acceleration and d is aquifer thickness. Because none of the other parameters are likely to change during an earthquake, changes in transmissivity are interpretable as changes in permeability. The values used are $\mu = 10^{-3}$ Pa s, $\rho = 10^3$ kg m^{-3}, $g = 9.8$ m s^{-2} and $d = 150$ m.

Received 21 November 2005; accepted 5 April 2006.

1. Rojstaczer, S. & Wolf, S. Permeability changes associated with large earthquakes: An example from Loma Prieta, California. *Geology* **20,** 211–214 (1992).
2. Muir-Wood, R. & King, G. Hydrological signatures of earthquake strain. *J. Geophys. Res.* **98,** 22035–22068 (1993).
3. Roeloffs, E. Poroelastic techniques in the study of earthquakes-related hydrologic phenomena. *Adv. Geophys.* **37,** 135–195 (1996).
4. Matsumoto, N. Regression-analysis for anomalous changes of ground-water level due to earthquakes. *Geophys. Res. Lett.* **19,** 1193–1196 (1992).
5. Brodsky, E. E., Roeloffs, E., Woodcock, D., Gall, I. & Manga, M. A mechanism for sustained groundwater pressure changes induced by distant earthquakes. *J. Geophys. Res.* **108**, doi:10.1029/2002JB002321 (2003).
6. Montgomery, D. & Manga, M. Stream flow and water well responses to earthquakes. *Science* **300,** 2047–2049 (2003).
7. Manga, M., Brodsky, E. E. & Boone, M. Response of stream flow to multiple earthquakes. *Geophys. Res. Lett.* **30**, doi:10.1029/2002GL016618 (2003).
8. Kitagawa, Y., Fujimori, K. & Koizumi, N. Temporal change in permeability of the rock estimated from repeated water injection experiments near the Nojima fault in Awaji Island, Japan. *Geophys. Res. Lett.* **29**, doi:10.1029/2001GL014030 (2002).
9. Hsieh, P., Bredehoeft, J. & Farr, J. Determination of aquifer transmissivity from earthtide analysis. *Water Resour. Res.* **23,** 1824–1832 (1987).
10. Raleigh, C., Healy, J. & Bredehoeft, J. An experiment in earthquake control at Rangely, Colorado. *Science* **191,** 1230–1237 (1976).
11. Bower, D. R. & Heaton, K. C. Response of an aquifer near Ottawa to tidal forcing and the Alaskan earthquake of 1964. *Can. J. Earth Sci.* **15,** 331–340 (1978).
12. Davis, E. E. & Elderfield, H. *Hydrogeology of the Oceanic Lithosphere* Fig. 8.16 (Cambridge Univ. Press, Cambridge, UK, 2004).
13. Wyatt, F. Displacement of surface monuments: horizontal motion. *J. Geophys. Res.* **87,** 979–989 (1982).
14. Love, A. E. H. *Mathematical Theory of Elasticity* 298 (Cambridge Univ. Press, Cambridge, UK, 1927).
15. Coble, R. The effects of the Alaskan earthquake of March 27, 1964, on ground water in Iowa. *Iowa Acad. Sci.* **72,** 323–332 (1965).
16. King, C. Y., Azuma, S., Igarashi, G., Ohno, M., Saito, H. & Wakita, H. Earthquake-related water-level changes at 16 closely clustered wells in Tono, Central Japan. *J. Geophys. Res.* **104,** 13073–13082 (1999).

17. Brace, W. A note on permeability changes in geologic material due to stress. *Pure Appl. Geophys.* **116,** 627–633 (1978).
18. Beresnev, I. A. & Johnson, P. A. Elastic-wave stimulation of oil production: A review of methods and results. *Geophysics* **85,** 1000–1017 (1994).
19. Bower, D. R. Bedrock fracture parameters from the interpretation of well tides. *J. Geophys. Res.* **88,** 5025–5035 (1983).
20. Cooper, H., Bredeheoft, J., Papadopulos, I. & Bennett, R. The response of well-aquifer systems to seismic waves. *J. Geophys. Res.* **70,** 3915–3926 (1965).
21. Kanamori, H. *et al.* Determinations of earthquake energy release and M_L using Terrascope. *Bull. Seismol. Soc. Am.* **83,** 330–346 (1993).
22. Hardebeck, J. L. & Shearer, P. M. Using s/p amplitude ratios to constrain the focal mechanisms of small earthquakes. *Bull. Seismol. Soc. Am.* **93,** 2434–2444 (2003).

Supplementary Information is linked to the online version of the paper at www.nature.com/nature.

Acknowledgements These measurements would not have been available without the long-term support of the PFO by the NSF, SCEC, the Vetlesen fund of the Scripps Institution, and the US Geological Survey; and the efforts of F. Wyatt, L. Weuve, S. Bralla, and S. Docktor. We gratefully acknowledge comments and discussion from E. Cochran, P. Davis, Z. Peng, A. Sagy and J. Vidale. J.E.E. was supported by a CIED scholarship and an NSF award.

Author Information Reprints and permissions information is available at npg.nature.com/reprintsandpermissions. The authors declare no competing financial interests. Correspondence and requests for materials should be addressed to J.E.E. (elkhoury@ess.ucla.edu).